Transient-State Kinetics of the ADP-Insensitive Phosphoenzyme in Sarcoplasmic Reticulum: Implications for Transient-State Calcium Translocation

Jeffrey P. Froehlich* and Phillip F. Heller

Laboratory of Molecular Aging, National Institute on Aging, National Institutes of Health, Gerontology Research Center,† Baltimore City Hospitals, Baltimore, Maryland 21224
Received November 9, 1983; Revised Manuscript Received July 27, 1984

ABSTRACT: The kinetics of formation of the ADP-sensitive (EP) and ADP-insensitive (E*P) phosphoenzyme intermediates of the CaATPase in sarcoplasmic reticulum (SR) were investigated by means of the quenched-flow technique. At 21 °C, addition of saturating ADP to SR vesicles phosphorylated for 116 ms with 10 μM ATP gave a triphasic pattern of dephosphorylation in which EP and E*P accounted for 33% and 60% of the total phosphoenzyme, respectively. Inorganic phosphate (P_i) release was less than stoichiometric with respect to E*P decay and was not increased by preincubation with Ca^{2+} ionophore. The fraction of E*P present after only 6 ms of phosphoenzyme formation was similar to that at 116 ms, indicating that isomerization of EP to E*P occurs very rapidly. Comparison of the time course of E*P formation with intravesicular Ca^{2+} accumulation measured by quenching with ethylene glycol bis(β-aminoethyl ether)-*N,N,N',N'*-tetraacetic acid + ADP revealed that Ca^{2+} release on the inside of the vesicle was delayed with respect to E*P formation. Since Ca^{2+} should dissociate rapidly dissociation from the low-affinity transport sites, these results suggest that Ca^{2+} remains "occluded" after phosphoenzyme isomerization and that a subsequent slow transition controls the rate of Ca^{2+} release at the intravesicular membrane surface. Analysis of the forward and reverse rate constants for the EP to E*P transition gave an expected steady-state distribution of phosphoenzymes strongly favoring the ADP-insensitive form. In contrast, the observed ratio of EP to E*P was about 1:2. To account for this discrepancy, a mechanism is proposed in which stabilization of the ADP-sensitive phosphoenzyme is brought about by a conformational interaction between adjacent subunits in a dimer.

Isolated vesicles of sarcoplasmic reticulum (SR)[1] carry out Ca^{2+}-dependent ATP hydrolysis by a mechanism which is believed to include the following steps (Scheme I) (Tada et al., 1978; de Meis, 1981). By convention, the states that bind Ca^{2+} with low affinity are indicated with asterisks. In the presence of micromolar Ca^{2+} levels, phosphorylation of the enzyme by ATP (step 2) leads to the formation of a phosphoenzyme (step 3) that is sensitive to ADP (Makinose, 1969; Kanazawa et al., 1971; Shigekawa et al., 1978; Shigekawa & Dougherty, 1978). A conformational change in the protein (step 4) converts the ADP-sensitive phosphoenzyme to an ADP-insensitive form (Bastide et al., 1973) which binds Ca^{2+} much less tightly than its precursor (Yamada & Tonomura, 1972; Makinose, 1973; Ikemoto, 1975, 1976; Takisawa & Makinose, 1983). Following phosphoenzyme conversion, the enzyme is dephosphorylated (steps 6 and 7) and undergoes a second conformational change (step 8) which increases its affinity for Ca^{2+}. In the absence of Ca^{2+}, the enzyme reacts with P_i to form a phosphoenzyme that is insensitive to ADP (Masuda & de Meis, 1973; Kanazawa & Boyer, 1973). Upon addition of millimolar Ca^{2+} (Ca^{2+} jump conditions), this ADP-insensitive phosphoenzyme is converted to a form that will react with ADP to form ATP (Knowles & Racker, 1975; de Meis & Tume, 1977).

Scheme I

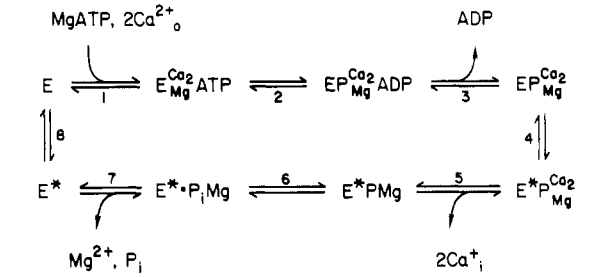

Various methods have been used to resolve the kinetics of the initial events associated with Ca^{2+} translocation including EGTA quenching (Sumida & Tonomura, 1974; Kurzmack et al., 1977; Ikemoto et al., 1981a,b), rapid Millipore filtration (Dupont, 1980, 1981), and optical monitoring with Ca^{2+}-sensitive dyes (Takisawa & Makinose, 1981; Pierce et al., 1983). Results of these studies have shown that Ca^{2+} accumulation is biphasic and that the initial phase, which coincides with phosphoenzyme formation, results in Ca^{2+} occlusion. The kinetics of this reaction are fast compared to the rate at which Ca^{2+} is released on the inside of the vesicle (Dupont, 1980; Chiu & Haynes, 1980), implying that the Ca^{2+} translocation sequence includes a slow transformation. Evidence linking this transformation to phosphoenzyme isomerization was recently obtained by Takisawa & Makinose (1983), who found an

† The Gerontology Research Center is fully accredited by the American Association for Accreditation of Laboratory Animal Care.

[1] Abbreviations: SR, sarcoplasmic reticulum; ATP, adenosine 5'-triphosphate; EGTA, ethylene glycol bis(β-aminoethyl ether)-*N,N,N',N'*-tetraacetic acid; EP, ADP-sensitive phosphoenzyme; E*P, ADP-insensitive phosphoenzyme; EP_r, residual phosphoenzyme; ANS, 8-anilino-1-naphthalenesulfonate; Tris, tris(hydroxymethyl)aminomethane; MOPS, 3-(*N*-morpholino)propanesulfonic acid.

approximate time-dependent correlation between Ca^{2+} release and ADP-insensitive phosphoenzyme formation in the deoxycholate-solubilized enzyme. Although detergent was used in order to facilitate resolution of the Ca^{2+} transients associated with phosphoenzyme formation, it may have affected the results since solubilization has been shown to alter the kinetics of slow reactions that regulate turnover of the system (Inesi et al., 1982; Kosk-Kosicka et al., 1983).

In the present study, the sequence of events mediating Ca^{2+} translocation was investigated by comparing the transient time courses of phosphoenzyme formation, P_i liberation, and intravesicular Ca^{2+} accumulation in native SR vesicles. The kinetics of formation of the ADP-insensitive phosphoenzyme were evaluated from the pattern of dephosphorylation resulting from the addition of saturating ADP at various times after initiating phosphorylation with ATP. According to Scheme I, the CaATPase reaction cycle includes three ADP-insensitive intermediates, one of which ($EP^{Ca_2}_{Mg}ADP$) occurs before the isomerization step. By simultaneously adding millimolar Ca^{2+} and ADP to phosphorylated vesicles, we were able to distinguish this intermediate from E*PMg which exhibits an increased rate of breakdown (due to reversal of steps 2–5) at high Ca^{2+} concentrations. The time dependence of E*PMg formation determined in the acid quench experiments was compared to the initial time course of intravesicular Ca^{2+} accumulation measured by terminating Ca^{2+} uptake with EGTA + ADP (Sumida & Tonomura, 1974). The results show that E*PMg is formed very rapidly, whereas intravesicular Ca^{2+} accumulation occurs more slowly, suggesting that release of occluded Ca^{2+} from the phosphorylated enzyme is rate limiting during Ca^{2+} translocation. Some of these results have previously appeared in abstract form (Froehlich et al., 1981).

Materials and Methods

Materials. All reagents were analytical grade. Disodium ATP and ADP, Tris–ATP and –ADP, and EGTA were purchased from Sigma. The Ca^{2+} ionophore A23187 was obtained from Boehringer Mannheim. $^{45}CaCl_2$ and [γ-^{32}P]-ATP were obtained from New England Nuclear. Solutions were prepared in once distilled, deionized water which contained approximately 5 μM Ca^{2+}.

Preparation of Membrane Vesicles. Sarcoplasmic reticulum vesicles were prepared from rabbit skeletal muscle as previously described (Froehlich & Taylor, 1975). Vesicles were either used immediately after preparation or quick-frozen in liquid nitrogen and stored at −80 °C. Freshly prepared vesicles loaded with 1 mM $^{45}CaCl_2$ and diluted into 5 mM EGTA exhibited passive Ca^{2+} efflux rates between 0.002 and 0.005 s^{-1} at 21 °C. Protein concentrations were determined by the method of Lowry et al. (1951).

Measurement of Phosphoenzyme Formation and Decomposition. Rapid mixing studies were carried out using the quenched-flow apparatus described by Froehlich et al. (1976). Unless otherwise indicated, SR vesicles (0.25 mg/mL) were phosphorylated at 21 °C in a medium containing 10 μM [γ-^{32}P]ATP, 100 mM KCl, 3 mM $MgCl_2$, 0.1 mM $CaCl_2$, 0.1 mM EGTA, and 20 mM Tris–maleate at pH 6.8. After a variable time delay, phosphoenzyme formation and P_i liberation were terminated by the addition of 3% perchloric acid + 2 mM H_3PO_4 (final concentrations). ^{32}P-Phosphoenzyme and [^{32}P]P_i were assayed according to previously described methods (Sumida et al., 1980).

Prior to measuring the kinetics of dephosphorylation, it was necessary to determine the level of ADP that produces saturation. For this purpose, SR vesicles phosphorylated for 116 ms as described above were dephosphorylated by the addition of a solution containing 100 mM KCl, 3 mM $MgCl_2$, 20 mM Tris–maleate, pH 6.8, and various concentrations of ADP ranging from 0 to 4 mM. The phosphoenzyme level remaining 542 ms after the start of dephosphorylation decreased with increasing [ADP] up to 1 mM ADP. Unless otherwise indicated, the phosphorylation conditions used in the dephosphorylation experiments were identical with those described above. Dephosphorylation by ADP was initiated by mixing 2 volumes of the reaction mixture containing phosphorylated vesicles with 1 volume of a solution containing 5 mM ADP, 100 mM KCl, 3 mM $MgCl_2$, 0.1 mM $CaCl_2$, 0.1 mM EGTA, and 20 mM Tris–maleate, pH 6.8. In the Ca^{2+} jump experiments, the dephosphorylation medium contained 15 mM $CaCl_2$ instead of 0.1 mM $CaCl_2$, all other conditions being the same. To increase the accessibility of transport sites on the phosphorylated carrier to Ca^{2+}, 0.5 mg of vesicles in 1 mL of buffered medium was preincubated with A23187 dissolved in absolute ethanol (1 mg of ionophore/mL of ethanol). In some experiments, the spontaneous decay of labeled phosphoenzyme was measured following a chase with unlabeled ATP or EGTA. Dephosphorylation was terminated after a variable time delay by the addition of 2.25% perchloric acid containing 2 mM H_3PO_4 (final concentrations).

Determination of Active Ca^{2+} Accumulation in Tightly Sealed and Ionophore-Treated Vesicles. The transient time course of ATP-dependent $^{45}Ca^{2+}$ accumulation by SR vesicles was determined by using EGTA or EGTA + ADP to terminate the transport reaction (Sumida & Tonomura, 1974). Uptake of $^{45}Ca^{2+}$ was initiated by mixing freshly prepared SR vesicles (0.5 mg/mL) suspended in a medium containing 100 mM KCl, 3 mM $MgCl_2$, and 20 mM Tris–maleate, pH 6.8, with an equal volume of the same solution but without vesicles and with 0.1 mM $^{45}CaCl_2$ and 20 μM ATP added. After a preset time interval, Ca^{2+} uptake was stopped by the addition of 2.5 mM EGTA or 2.5 mM EGTA + 1 mM ADP (final concentrations). Vesicles in a 0.5-mL aliquot of the quenched reaction mixture were collected on a 0.45-μm Millipore filter and washed with 10 mL of 1 mM EGTA, 100 mM KCl, and 20 mM Tris–maleate, pH 6.8. The filters were air-dried, and the radioactivity was determined by liquid scintillation counting. Although we were unable to detect Ca^{2+} retention by ionophore-treated vesicles using the manual filtration technique, small amounts of Ca^{2+} may have been trapped inside the vesicles and lost during the subsequent filtration and washing procedures. To test this possibility, A23187-treated vesicles were mixed in an Aminco-Morrow stopped-flow device with a solution containing 500 μM ATP, 20 μM $CaCl_2$, 1 mM $MgCl_2$, 50 mM KCl, 20 mM MOPS, pH 6.8, and 30 μM arsenazo III to monitor Ca^{2+} uptake. Since the initial trace showed no evidence of Ca^{2+} accumulation, these vesicles are unlikely to retain significant amounts of Ca^{2+} during ATP hydrolysis.

Computer Simulation of the Dephosphorylation Reaction. The kinetic constants of the ATPase partial reactions were determined by computer simulation of the dephosphorylation time course using a nonlinear, least-squares curve-fitting routine (Knott, 1979). The interaction between Ca^{2+} and the low-affinity sites on the ADP-insensitive phosphoenzyme was analyzed by computer fitting the Ca^{2+} titration data to the Hill equation after making an appropriate correction for the amount of Ca^{2+} bound to ADP (Bulos & Sacktor, 1979).

Results

Dephosphorylation by ADP of the Phosphoenzyme Formed in the Steady State. According to Scheme I, conditions which

Table I: Effect of Jumping [Ca^{2+}] and [Mg^{2+}] on the Kinetics of the ADP-Induced Dephosphorylation Reaction[a]

dephosphorylation condn	phosphorylation time (ms)	[EP] (nmol/mg)	[E*P] (nmol/mg)	[EP_r] (nmol/mg)	k (s^{-1})	$\Delta[P_i]$ (nmol/mg)
1.66 mM ADP	6	0.27	0.32	0.06	36	0.11
	10	0.44	0.53	0.11	21	0.14
	116	0.76	1.37	0.18	21	0.48
1.66 mM ADP + 5 mM $CaCl_2$[b]	6	0.29	0.30	0.15	144	0
	116	0.70	1.30	0.32	50	0.12
1.66 mM ADP + 20 mM $MgCl_2$	116	0.85	2.43	0.21	17	2.10

[a] SR vesicles (0.25 mg/mL) were preincubated with A23187 and phosphorylated as described under Materials and Methods. After 6, 10, or 116 ms of phosphoenzyme formation, 1.66 mM ADP, 1.66 mM ADP + 5 mM $CaCl_2$, or 1.66 mM ADP + 20 mM $MgCl_2$ (final concentrations) was added to the reaction mixture, and dephosphorylation was allowed to proceed for an additional variable time interval prior to mixing with acid. The levels of the ADP-sensitive (EP), ADP-insensitive (E*P), and residual (EP_r) phosphoenzymes and the rate constant for E*P decay, k, were estimated from semilogarithmic plots of phosphoenzyme concentration vs. time. The rate constant for EP decay could not be resolved but was estimated to be greater than 300 s^{-1}. The amount of the residual phosphoenzyme was assumed to be equivalent to the level of phosphoenzyme measured at 542 ms. $\Delta[P_i]$ represents the amount of phosphate released in the 542-ms interval between the start of dephosphorylation and addition of the acid quench. [b] The concentrations of EP and E*P were calculated by assuming that the rise in the level of EP_r due to the Ca^{2+} jump occurred instantaneously.[2]

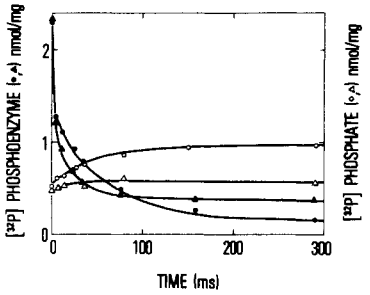

FIGURE 1: Phosphoenzyme decomposition and P_i release following the addition of ADP and ADP + Ca^{2+} (Ca^{2+} jump) to SR vesicles phosphorylated for 116 ms. SR vesicles (0.5 mg/mL) were pretreated with A23187 (see Materials and Methods) and phosphorylated in a medium containing 10 μM [γ-^{32}P]ATP, 100 mM KCl, 3 mM $MgCl_2$, 0.1 mM $CaCl_2$, 0.1 mM EGTA, and 20 mM Tris–maleate, pH 6.8. After 116 ms of phosphoenzyme formation, either (○, ●) 1.66 mM ADP or (△, ▲) 1.66 mM ADP + 5 mM $CaCl_2$ (final concentrations) was added, and dephosphorylation was allowed to proceed for the indicated times prior to the addition of acid. (●, ▲) Phosphoenzyme; (○, △) inorganic phosphate.

increase intravesicular [Ca^{2+}] will shift phosphoenzyme isomerization (step 4) in the direction of the ADP-sensitive phosphoenzyme by increasing the level of saturation of low-affinity Ca^{2+} binding sites on E*PMg. Unless otherwise indicated, membrane vesicles used in the ADP dephosphorylation experiments were pretreated with A23187 in order to prevent a Ca^{2+}-induced shift in the isomerization equilibrium.

Figure 1 (closed circles) shows the time course of phosphoenzyme decomposition following the addition of 1.66 mM ADP to SR vesicles phosphorylated for 116 ms in a medium containing 10 μM [γ-^{32}P]ATP, 3 mM $MgCl_2$, and 14 μM Ca^{2+}. The time elapsed between the first and second stages of mixing was sufficient to allow phosphorylation to reach a steady state (Figure 5). The initial time course of dephosphorylation exhibited a rapid phase ($k > 300$ s^{-1}) followed by a slower, time-resolved phase ($k = 21$ s^{-1}) which constituted 33% and 60% of the total phosphoenzyme, respectively (Table I). After 150 ms, there appeared an even slower phase ($k < 1$ s^{-1}) which accounted for the remaining phosphoenzyme and is hereafter referred to as the residual phosphoenzyme. Including 2.5 mM EGTA together with ADP in the final reaction mixture gave results that were similar to those obtained with ADP alone (not shown).

Inorganic phosphate production occurring during dephosphorylation (open circles, Figure 1) did not show a corresponding rapid phase, indicating that the initial disappearance of phosphoenzyme resulted from the transfer of enzyme-bound phosphate to ADP to form ATP (step 2, Scheme I). The initial rate of P_i liberation was similar to the rate of decomposition of the slow component; however, the total amount of P_i production was equal to about one-third of the simultaneous decay of the phosphoenzyme. A similar discrepancy between phosphoenzyme decay and P_i liberation was observed in vesicles that had not been preincubated with ionophore prior to phosphorylation (not shown).

The absence of P_i liberation during the initial phase of dephosphorylation and its presence during the subsequent phase suggest that the rapid and slow phases correspond to dephosphorylation of the ADP-sensitive (EP) and ADP-insensitive (E*P) phosphoenzymes, respectively. Since P_i production was less than stoichiometric with respect to E*P decay, significant conversion of E*P to EP and then to EATP probably occurred under these conditions, despite the presence of the ionophore. Under these conditions, the observed rate of E*P decay, 21 s^{-1}, equals the sum of the rate constants for E*P decomposition in the forward and reverse directions so that the back-transition will have a rate less than 21 s^{-1}. To determine if ADP-induced E*P decomposition could be accelerated by a Ca^{2+} jump, the experiment was repeated using 1.66 mM ADP + 5 mM $CaCl_2$ to initiate dephosphorylation. As seen in Figure 1, raising the Ca^{2+} level during dephosphorylation increased the rate of E*P decay (closed triangles) and the initial rate of P_i release (open triangles) while decreasing total P_i production compared to the previous experiment. Thus, increasing the level of saturation of the low-affinity sites on E*P led to an increased rate of conversion of E*P to EP and ATP synthesis while simultaneously reducing the rate of E*P breakdown in the direction of P_i. An additional effect noted was a 2-fold increase in the level of the residual phosphoenzyme (Table I) which may have resulted from competition between Ca^{2+} and K^+ or Mg^{2+} for the cation binding sites activating E*P hydrolysis (Shigekawa & Akowitz, 1979; Yamada & Ikemoto, 1980). When the contribution of the residual phosphoenzyme (about 15% of the total phosphoenzyme) was subtracted from the decay curve, the remaining time points (with the exception of the zero-time point) fell on a straight line with a slope of 50 s^{-1} (Figure 2).[2] The fact that 85% of the phosphoenzyme in the slow phase showed an accelerated rate of decay in the presence of a Ca^{2+} jump

[2] The method used to calculate the slope of E*P is based on the assumption that the increase in [EP_r] resulting from the Ca^{2+} jump occurs instantaneously. A slow time-dependent increase in [EP_r] would introduce a larger difference between [EP_r] and the early time points, resulting in a steeper slope and a correspondingly larger rate constant. Consequently, the calculated rate constant obtained from the semilog plot may underestimate the true value.

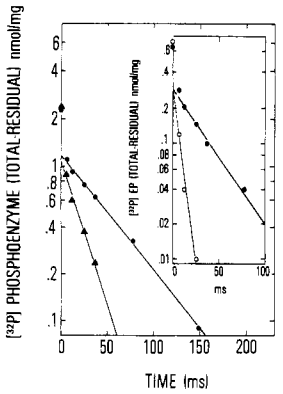

FIGURE 2: Semilogarithmic plots of ADP-induced and ADP + Ca^{2+} induced dephosphorylation at 6 and 116 ms of phosphoenzyme formation. The time courses of phosphoenzyme decay for the experiments shown in Figure 1 (116 ms of phosphorylation) were plotted semilogarithmically after subtraction of the residual phosphoenzyme level reported in column 5 of Table I. Phosphoenzyme decay (●) in the absence or (▲) in the presence of a Ca^{2+} jump. Inset: Semilogarithmic plots of phosphoenzyme concentration vs. time for the dephosphorylation experiments shown in Figure 3 (6 ms of phosphorylation). The residual phosphoenzyme was subtracted from each of the earlier time points. Phosphoenzyme decay (●) in the absence or (○) in the presence of a Ca^{2+} jump.

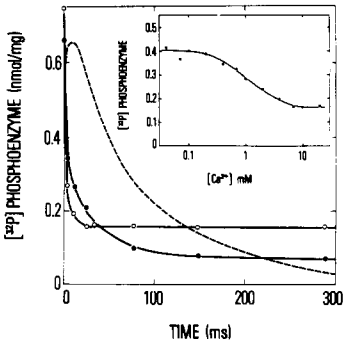

FIGURE 3: Time courses of dephosphorylation resulting from the addition of ADP or ADP + Ca^{2+} (Ca^{2+} jump) following 6 ms of phosphoenzyme formation. Ionophore-treated SR vesicles were phosphorylated for 6 ms and dephosphorylated as described in the legend to Figure 1. The dashed line represents the simulated time course of dephosphorylation using the scheme given in the legend to Table VI and rate constants given in column 3 of Table VI except that k_{-1} = 35 s^{-1} (see Simulation of the ADP-Induced Dephosphorylation Time Course under Results). The difference between the zero-time levels for the real and simulated curves equals the residual phosphoenzyme, EP_r, which was subtracted from the data points prior to simulation. Phosphoenzyme decay (●) in the absence or (○) in the presence of a Ca^{2+} jump. The inset shows the level of phosphoenzyme remaining 6 ms after the addition of ADP + Ca^{2+} as a function of the final [Ca^{2+}] present in the reaction medium. SR vesicles were phosphorylated by ATP in the presence of 20 μM Ca^{2+} (see Materials and Methods), and after 6 ms, 1.66 mM ADP was added together with sufficient additional Ca^{2+} to bring the final concentration to the levels indicated in the figure. Phosphoenzyme decay was allowed to proceed for 6 ms prior to addition of the acid quench.

lends support to our previous conclusion that dephosphorylation during the slow phase is due primarily to the breakdown of E*P.

In contrast to the effects produced by the Ca^{2+} jump, raising the Mg^{2+} level during dephosphorylation had no effect on the rate of E*P decay or rate of concomitant P_i liberation (Table I). However, the amount of P_i liberated during dephosphorylation increased, becoming nearly stoichiometric with respect to E*P decay.

Dephosphorylation by ADP during the Transient State of Phosphorylation. From the results of the experiment in Figure 1, one might expect to find most of the phosphoenzyme in the ADP-sensitive form during the early stages of phosphorylation since rapid conversion of EP to E*P in the presence of a slow back-transition (<21 s^{-1}) would virtually deplete the system of EP by 116 ms. In the experiment shown in Figure 3 (closed circles), conditions identical with those in Figure 1 were employed except that the time delay prior to the addition of ADP was reduced to 6 ms. As expected, the predominant effect of decreasing the phosphorylation time was to decrease the total amount of phosphoenzyme. However, E*P still accounted for about half of the total phosphoenzyme, indicating that EP was rapidly being converted to E*P. In addition, the quantity of P_i liberated during dephosphorylation was equal to about one-third of the ADP-insensitive phosphoenzyme (Table I). The less than stoichiometric P_i release observed in this and the dephosphorylation experiment at 116 ms (Figure 1) was unexpected since ionophore-treated vesicles were unable to retain Ca^{2+} under active loading conditions (see Materials and Methods) and because high concentrations of Ca^{2+} (~1 mM; see below) are necessary to activate reversal of the phosphoenzyme transition. This suggests that the transport system contains an ionophore-inaccessible compartment that is able to donate Ca^{2+} back to E*P following the addition of ADP.

Another species that might contribute to the slow phase of dephosphorylation is $EP^{Ca_2}_{MgADP}$, which is ADP insensitive because it contains bound ADP. If this intermediate is in rapid equilibrium with $E^{Ca_2}_{MgATP}$ (step 2), then slow dissociation of ATP from the catalytic site (step 1) will produce a correspondingly slow rate of disappearance of $EP^{Ca_2}_{MgADP}$ by shifting the equilibrium of step 2 to the left (Pickart & Jencks, 1982).

However, if the slow phase of dephosphorylation was due entirely to a shift in the phosphorylation equilibrium during that phase, then P_i production should not have occurred. Moreover, $EP^{Ca_2}_{MgADP}$ should not exhibit an increased rate of decay following a Ca^{2+} jump because the transport sites on this species contain tightly bound Ca^{2+} (Takakuwa & Kanazawa, 1979, 1982). When the Ca^{2+} concentration was increased during the second stage of mixing (open circles, Figure 3), the rate constant for E*P dephosphorylation rose from 35 to 144 s^{-1} while total P_i production fell below the limit of detection (Table I). As in the previous Ca^{2+} jump experiment, E*P decomposition could be described by a single exponential after subtraction of the residual phosphoenzyme. These results indicate that the slow phase of dephosphorylation measured after 6 ms of phosphorylation with ATP corresponds primarily to the breakdown of E*P.

Table II presents the results of a series of experiments in which the time of incubation with ATP was allowed to vary between 6 and 116 ms prior to the addition of ADP. To minimize the error introduced by using different enzyme preparations, the concentration of E*P was expressed as a fraction of the total phosphoenzyme concentration ($[EP]_{total}$) present at the start of dephosphorylation (column 2, Table II). The results show that a fairly constant ratio of [E*P] to $[EP]_{total}$ was maintained throughout the entire time course of phosphoenzyme formation, indicating that isomerization occurs rapidly following initiation of phosphorylation. This contrasts with the behavior at 0 °C in the absence of monovalent cations where a slow, time-dependent accumulation of E*P was observed (Shigekawa & Dougherty, 1978).

*Titration of the Ca^{2+} Site Activating the Conversion of EP to E*P.* Previous studies by Knowles & Racker (1975) and de Meis & Tume (1977) have shown that millimolar levels of Ca^{2+} are necessary to activate conversion of the phosphoenzyme formed from P_i to an ADP-sensitive form and stimulate the rate of ATP synthesis during ATP $\rightleftharpoons$ P_i exchange.

Table II: Kinetics of Formation of ADP-Insensitive Phosphoenzyme and Intravesicular $^{45}Ca^{2+}$ Accumulation[a]

phosphorylation time (ms)	E^*P/EP_0	$[EP]_{total}$ (nmol/mg)	$[E^*P]_{calcd}$ (nmol/mg)	$[P_i]$ (nmol/mg)	$[^{45}Ca^{2+}]$ (nmol/mg)
6	0.49	1.0	0.49	0.05	0.20
10	0.50	1.5	0.75	0.05	0.25
20	0.35	2.4	0.84	0.06	0.45
25	0.34	2.65	0.85	0.20	0.55
43	0.41	3.05	1.25	0.45	1.0
59	0.48	3.0	1.44	0.85	1.35
116	0.58	2.65	1.54	2.25	2.35

[a] The enzyme was phosphorylated with ATP for the different times given in column 1 and then dephosphorylated by ADP according to the conditions described in the legend to Figure 1. The level of ADP-insensitive phosphoenzyme, E*P, present at a given phosphorylation time was evaluated from a semilogarithmic plot of the time course of phosphoenzyme decomposition and expressed as a fraction of the amount of phosphoenzyme present at the start of dephosphorylation, EP_0 (column 2). The concentrations of EP_{total}, P_i, and intravesicular $^{45}Ca^{2+}$ listed in columns 3, 5, and 6 were obtained from the experiments shown in Figure 5. When the times listed in column 1 did not exactly coincide with those of Figure 5, the values for $[EP]_{total}$, $[P_i]$, and $[^{45}Ca^{2+}]$ were estimated from smooth curves drawn by eye through the existing data points. Each of the values listed in column 2 was multiplied by the corresponding value in column 3 to give the estimated level of ADP-insensitive phosphoenzyme, $[E^*P]_{calcd}$, at a given time, t (column 4). When these values were plotted as a function of phosphorylation time, they gave an exponential curve (dashed line, Figure 5) which represents the estimated time course of E*P formation for the phosphorylation experiment shown in Figure 5.

Table III: Hill Analysis of the Low-Affinity Ca^{2+} Binding Site Titration Data

exptl condn	phosphorylation time (ms)	$K_{0.5}$ (mM)	n
untreated vesicles[a]	6	0.89 ± 0.13	1.40 ± 0.19
	116	0.73 ± 0.18	0.94 ± 0.14
A23187-treated vesicles[b]	6	0.85 ± 0.12	1.40 ± 0.18
	116	0.60 ± 0.10	1.02 ± 0.14

[a] Tightly sealed SR vesicles (0.5 mg/mL), suspended in a medium containing 100 mM KCl, 3 mM $MgCl_2$, 20 mM $CaCl_2$, and 20 mM Tris–maleate, pH 6.8, were mixed with an equal volume of a solution containing the same components but without enzyme and with 20 μM [γ-^{32}P]ATP added. After 6 or 116 ms, the vesicles were dephosphorylated by the addition of 1.66 mM ADP and Ca^{2+} at (final) concentrations varying between 20 μM and 20 mM. The dephosphorylation time interval, measured from the time of addition of ADP + Ca^{2+} to the time of addition of the acid quench, was 6 ms. The Ca^{2+} concentration producing half-maximal activation of dephosphorylation, $K_{0.5}$, and the Hill coefficient, n, were determined by fitting the titration data to the Hill equation using a nonlinear least-squares curve-fitting procedure (MLAB). The parameter values are reported as best fit ± the standard error. [b] The Ca^{2+} titration experiments were identical with those described above except that the vesicles were preincubated with A23187.

Table IV: Effect of Pretreatment with the Ca^{2+} Ionophore A23187 on Dephosphorylation of SR Vesicles following the Addition of ADP or ADP plus Ca^{2+}[a]

dephosphorylation condn	phosphorylation time (ms)	phosphoenzyme level (nmol/mg)	Δ[E*P][b] (nmol/mg)
untreated SR			
+1.66 mM ADP	6	0.394 ± 0.002	
	116	0.840 ± 0.014	
+1.66 mM ADP + 5 mM $CaCl_2$	6	0.182 ± 0.006	0.212 ± 0.006
	116	0.520 ± 0.008	0.320 ± 0.016
A23187-treated SR			
+1.66 mM ADP	6	0.378 ± 0.007	
	116	1.20 ± 0.010	
+1.66 mM ADP + 5 mM $CaCl_2$	6	0.157 ± 0.003	0.221 ± 0.008
	116	0.817 ± 0.005	0.383 ± 0.011

[a] Freshly prepared SR vesicles were phosphorylated as described under Materials and Methods with or without pretreatment with A23187. After 6 or 116 ms of phosphorylation, either 1.66 mM ADP or 1.66 mM ADP + 5 mM $CaCl_2$ was added to the reaction mixture, and dephosphorylation was allowed to proceed for 13 ms prior to the addition of acid. The phosphoenzyme remaining after 13 ms corresponds primarily to E*P since the rapid phase of dephosphorylation is essentially over within 6 ms (Figures 1 and 3). Phosphoenzyme level is reported as the mean ± standard error. [b] The difference betweeen the phosphoenzyme levels (which include the residual component) obtained in the absence and presence of a Ca^{2+} jump, Δ[E*P], was used to measure the extent of activation by Ca^{2+} of E*P decomposition in tightly sealed and ionophore-treated vesicles. Evaluation of the differences between the corresponding values for Δ[E*P] in tightly sealed and ionophore-treated vesicles by the t test showed that they were not significant.

To measure the Ca^{2+} concentration dependence of the reverse phosphoenzyme transition, the ADP + Ca^{2+} jump experiment was repeated using different final Ca^{2+} levels (40 μM–20 mM) to activate dephosphorylation. Because this experiment involved determining the initial velocity at several different Ca^{2+} levels, it was convenient to monitor the initial response to Ca^{2+} by using the 6-ms time point which lies on the linear portion of the decay curve. As seen in the inset to Figure 3, activation of dephosphorylation of the ADP-insensitive phosphoenzyme showed a rather steep dependence on Ca^{2+} concentration, becoming saturated somewhere above 7 mM. At 6 ms, activation of the conversion of E*P to EP was half-maximal at 0.89 mM Ca^{2+} and exhibited a weak cooperative dependence on $[Ca^{2+}]$ (n = 1.40; Table III). Increasing the phosphorylation time from 6 to 116 ms reduced the value of the Hill coefficient (n) to 0.94 without significantly affecting the level of Ca^{2+} required for half-maximal activation. These results suggest that more than one Ca^{2+} binding site is involved in activation of dephosphorylation of the phosphoenzyme formed during the presteady state of ATP hydrolysis and that as more of the enzyme becomes phosphorylated the properties of the sites are modified such that they interact less cooperatively.

*Effect of Ionophore on Activation of E*P Decomposition by Ca^{2+}.* Although there is fairly good evidence linking Ca^{2+} translocation to phosphoenzyme isomerization, it is not clear at what stage in the transport cycle the carrier returns to the external surface after releasing Ca^{2+} internally. If the inside to outside carrier transition is coupled to the conversion of E* to E as suggested by Carvahlo et al. (1976), then a Ca^{2+} jump should not affect the rate of E*P decay in tightly sealed vesicles because the low-affinity sites will face the inner membrane surface and therefore will not be immediately available to bind Ca^{2+}. Table IV summarizes the results of experiments in which the sensitivity of E*P to an ADP + Ca^{2+} jump was compared in ionophore-treated and tightly sealed vesicles. As seen in the table, omission of the ionophore had essentially no effect on the extent of activation of dephosphorylation produced by adding Ca^{2+} simultaneously with ADP 6 or 116 ms after the start of phosphoenzyme formation. When the Ca^{2+} titration experiment shown in the inset to Figure 3 was re-

Table V: Effect of Ca^{2+} Jump on Inorganic Phosphate Release

exptl condn	v (nmol mg^{-1} s^{-1})
untreated vesicles[a]	
+5 mM EGTA	17
+5 mM $CaCl_2$	14
A23187-treated vesicles[b]	
+5 mM $CaCl_2$	4.2

[a] SR vesicles (0.5 mg/mL) were phosphorylated as described under Materials and Methods. After 116 ms, the vesicles were mixed with 5 mM EGTA or 5 mM $CaCl_2$ (final concentrations), and P_i liberation was measured at timed intervals varying between 6 and 289 ms. v represents the velocity of P_i liberation immediately following the addition of EGTA or $CaCl_2$. [b] Conditions were the same as those described above except that the vesicles were preincubated with A23187.

peated in the absence of A23187, the results were indistinguishable from those obtained with ionophore-treated vesicles (Table III).

The results of the ADP + Ca^{2+} jump experiments suggest that during Ca^{2+} translocation the low-affinity transport sites return to the extravesicular surface prior to E*P hydrolysis. If this interpretation is correct, then addition of Ca^{2+} without ADP should immediately inhibit P_i liberation by driving the Ca^{2+} dissociation reaction back in the direction of the loaded carrier (step 5, Scheme I). Alternatively, when ADP binds to the carrier, it may trigger a conformational change that exposes the transport sites to the external medium. To test this hypothesis, tightly sealed vesicles were phosphorylated for 116 ms with 10 μM ATP and then mixed with 5 mM $CaCl_2$ prior to measuring phosphorylation and P_i liberation. In a control experiment, 5 mM EGTA was added to phosphorylated vesicles in order to measure the spontaneous rate of E*P hydrolysis. The results of these experiments, summarized in Table V, show that the rate of P_i liberation immediately following the addition of Ca^{2+} to nonleaky vesicles was similar to that found in SR mixed with EGTA. When this experiment was repeated with ionophore-treated vesicles, jumping the Ca^{2+} concentration reduced the initial rate of P_i liberation to 25% of the control value, indicating stabilization of E*P by Ca^{2+}. In tight vesicles, the initial rates of phosphoenzyme decay were similar in both the Ca^{2+} jump and control experiments, whereas ionophore treatment strongly inhibited phosphoenzyme decay following the Ca^{2+} jump (not shown). These results indicate that in the absence of added ADP the low-affinity Ca^{2+} binding sites on E*P face the inside of the vesicle and that the inside to outside carrier transition takes place after E*P hydrolysis.

Decomposition of the Phosphoenzyme following a Chase with EGTA or ATP. Figure 4 shows an experiment in which the enzyme was phosphorylated for 6 ms under conditions identical with those in Figure 1 and then chased with 5 mM unlabeled ATP. In contrast to the results obtained with ADP, the dephosphorylation time course showed a brief initial rise followed by an exponential decay. Since the presence of a 1000-fold excess of unlabeled substrate should have prevented further binding of labeled ATP, the initial rise in phosphoenzyme suggests that the system contains a pool of bound nucleotide that is not readily exchangeable with free ATP in the medium (Shigekawa & Kanazawa, 1982). When cold ATP was added to the phosphoenzyme after 116 ms (inset, Figure 4), the curve that remained after subtraction of the residual phosphoenzyme (about 10% of the total phosphoenzyme) showed a monophasic decay pattern with an apparent rate constant of 28 s^{-1}. More than 90% of the phosphoenzyme decayed to P_i, indicating that the ATP chase contained very little ADP contamination. Using 5 mM EGTA together with 5 mM ATP to chase the phosphoenzyme gave results that were

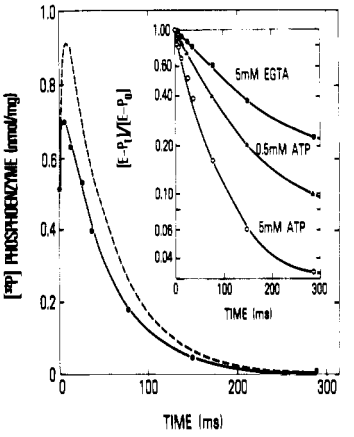

FIGURE 4: Time course of dephosphorylation following a chase with EGTA or unlabeled ATP. SR vesicles (0.5 mg/mL) were phosphorylated for 6 ms and then dephosphorylated by the addition of 5 mM unlabeled ATP (final concentration). The residual phosphoenzyme (0.2 nmol/mg) was subtracted from each of the earlier time points shown in the figure. The dashed curve represents the predicted time course of phosphoenzyme decay following an ATP chase simulated by using the scheme given in the legend to Table VI and the rate constants listed in column 2 of Table VI (except that k_5 = 30 s^{-1}) and by adjusting k_1 = 0 after allowing phosphoenzyme to accumulate for 6 ms. The initial ATP concentration was 10 μM. The solid curve was obtained by using the same set of rate constants except that the rate constant for ATP dissociation (k_{-1}) was 250 s^{-1}. The inset shows the normalized time courses of dephosphorylation produced by chasing with EGTA or ATP 116 ms after initiating phosphorylation with labeled ATP. The phosphorylation conditions were identical with those described above. Dephosphorylation was initiated by the addition of (●) 5 mM EGTA, (△) 0.5 mM unlabeled ATP, or (○) 5 mM unlabeled ATP (final concentrations) in a medium containing 100 mM KCl, 3 mM $MgCl_2$, and 20 mM Tris–maleate, pH 6.8. The abbreviations on the vertical axis are as follows: $[E\text{-}P_0]_t$, phosphoenzyme level present at 116 ms (when the chase was added); $[E\text{-}P_t]$, phosphoenzyme level measured at time t after the addition of the chase.

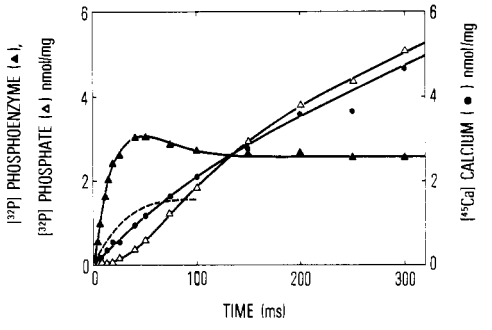

FIGURE 5: Pre-steady-state time courses of phosphoenzyme formation, intravesicular $^{45}Ca^{2+}$ accumulation, and P_i release. SR vesicles (0.25 mg/mL) were phosphorylated in a medium containing 100 mM KCl, 3 mM $MgCl_2$, 20 mM Tris–maleate, pH 6.8, and either (▲, △) 10 μM [γ-^{32}P]ATP + 0.1 mM $CaCl_2$ + 0.1 mM EGTA or (●) 10 μM ATP + 0.1 mM $^{45}CaCl_2$. At the indicated times, the reaction was terminated by the addition of either (▲, △) 2.25% perchloric acid + 2 mM H_3PO_4 or (●) 2.5 mM EGTA + 1 mM ADP. (▲) Phosphoenzyme formation; (△) P_i release; (●) intravesicular Ca^{2+} accumulation. The dashed line represents the approximate time course of formation of the ADP-insensitive phosphoenzyme constructed from the values of $[E^*P]_{calcd}$ given in column 4 of Table II.

similar to those obtained with 5 mM ATP alone. Decreasing the concentration of the ATP chase from 5 to 0.5 mM produced a biphasic decay pattern (inset, Figure 4) with a slower initial rate constant (15 s^{-1}), while chasing with 5 mM EGTA reduced the initial rate of dephosphorylation to 10 s^{-1}.

The dephosphorylation time course following the addition of 5 mM EGTA was more complex than the pattern resulting from the chase with 5 mM ATP (inset, Figure 4). After 149 ms of exposure to EGTA, the rate of dephosphorylation began

Table VI: Computer Simulation of Phosphoenzyme Formation and Decomposition[a]

rate constants, forward/reverse	phosphoenzyme formation	phosphoenzyme decomposition at	
		6 ms	116 ms
k_1/k_{-1}	$(1 \times 10^7)/35$	$(1 \times 10^7)/3000$	$(1 \times 10^7)/35$
k_2/k_{-2}	180/400	180/400	180/400
k_3/k_{-3}	$1000/(1 \times 10^7)$	$1000/(1 \times 10^7)$	$1000/(1 \times 10^7)$
k_4/k_{-4}	500/20	500/20 (200)	30/10 (80)
k_5/k_{-5}	15/5	15/5	15/5
k_6/k_{-6}	10/0	10/0	10/0

[a] Rate constants controlling the formation and breakdown of the ADP-sensitive (EP) and ADP-insensitive (E*P) phosphoenzymes were obtained by simulation of the time course of ADP-induced dephosphorylation by using the following scheme:

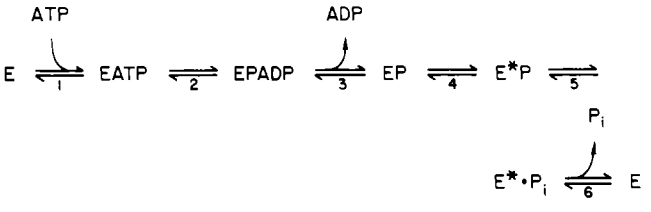

In this scheme, the outside to inside carrier transition and Ca^{2+} release from E*P were combined into a single step, EP ⇌ E*P. Prior to modeling the ADP dephosphorylation data, we subtracted the residual phosphoenzyme from each of the data points.[2] Phosphoenzyme formation was simulated by using the rate constants given in column 1, an initial ATP concentration of 10 μM, and a total site concentration of 1 μM. Dephosphorylation after 6 or 116 ms of phosphoenzyme formation was simulated by redefining the initial conditions so that [ADP] = 2 mM and $k_1 = 0$ and by setting the remaining rate constants equal to the values given in columns 3 and 4. To simulate ADP-induced dephosphorylation in the presence of a Ca^{2+} jump, k_4 was increased at the start of dephosphorylation to the values shown in parentheses (columns 3 and 4). The dashed curve in Figure 3 represents the simulated time course of ADP-induced dephosphorylation at 6 ms obtained by adjusting k_{-1} to 35 s^{-1} and the remaining constants to the values given in column 3. The observed phosphoenzyme level equals the sum of the acid-stable phosphorylated states (EPADP + EP + E*P). Units of k_1 and k_{-3} are in M^{-1} s^{-1}. All other rate constants are in s^{-1}.

to decline, indicating the presence of a second major component [cf. Figure 5; Sumida et al., 1980]. At even longer time intervals, a residual component, accounting for about 10% of the total phosphoenzyme, was observed (not shown). A close approximation to the dephosphorylation time course without the residual component was obtained by using a decay function consisting of two exponentials with rate constants of 11.5 and the 6.7 s^{-1}. Because these values are both smaller than the single rate constant obtained with 5 mM ATP + EGTA or 5 mM ATP alone, it appears that ATP accelerates both phases of the EGTA-induced dephosphorylation reaction.

Simulation of the ADP-Induced Dephosphorylation Time Course. The results of the experiments in Figure 3 and Table I suggest that the ADP dissociation and phosphoenzyme isomerization take place very rapidly following transphosphorylation. In principle, this information can be used to assign lower limits to the rate constants for ADP dissociation and the reactions of the translocation sequence. For evaluation of these constants, we resorted to computer simulation of the ADP dephosphorylation time course using a condensed version of the reaction mechanism given in the introduction (see Table VI footnote). Because there was insufficient data to separately define the rate constants corresponding to the isomerization reaction and the carrier transition, these steps were combined into a single step, EP ⇌ E*P where E*P represents the sum of the ADP-insensitive intermediates ($E^*P^{Ca_2}_{Mg}$ + E*PMg) in Scheme I. Using this approximation, we obtained a minimum overall rate constant of 350 s^{-1} for the steps involving ADP release and phosphoenzyme conversion. Further separation of these rate constants was achieved by simultation of the time course of dephosphorylation obtained at less than saturating levels of ADP.[3] This gave a minimum rate constant for the conversion of EP to E*P of 500 s^{-1}. An estimate of the rate constant for the reverse transition (E*P → EP) at low Ca^{2+} levels was obtained by subtracting the rate of phosphoenzyme decay in the presence of EGTA from the ADP-induced rate of E*P breakdown. EGTA favors E*P decay in the forward direction as evidenced by the stoichiometric relationship between dephosphorylation and P_i releae (Sumida et al., 1980). In the presence of saturating ADP levels, however, combination of EP with ADP will irreversibly pull the isomerization reaction (step 4) back in the direction of $EP^{Ca_2}_{MgADP}$:

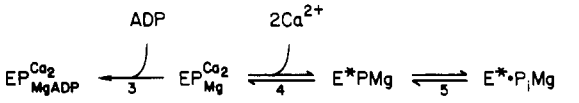

E*PMg will decay in both directions, and its rate of disappearance, 20–35 s^{-1} (Table I), is equal to the sum of the rate constants corresponding to the forward (k_5) and reverse (k_{-4}) reactions (Frost & Pearson, 1965). Because E*P is hydrolyzed to P_i in the presence of EGTA at a rate of 10 s^{-1} (k_5), the apparent rate of conversion of E*P to EP equals 10–25 s^{-1} (k_{-4}). From the values for the rate constants for the forward (500 s^{-1}) and reverse (10–25 s^{-1}) phosphoenzyme transitions and the overall CaATPase activity (11 nmol mg^{-1} s^{-1}; Figure 5), it can be shown that less than 10% of the phosphoenzyme in the steady state should be ADP sensitive. In contrast, the observed decay pattern (Figure 1) revealed that EP accounted for about one-third of the total phosphoenzyme, indicating that some constraint prevents the isomerization reaction from going to completion.

We previously showed (Sumida et al., 1980) that in order to fit the ATP concentration dependence of phosphoenzyme formation at low ATP levels, it was necessary to assign a low value (~35 s^{-1}) to the rate constant for ATP dissociation. This, together with the high rate of ATP binding (1×10^7 M^{-1} s^{-1}), will lead to a transient buildup of bound [γ-^{32}P]ATP which will continue to phosphorylate the enzyme following dilution of the labeled substrate with cold ATP. Consistent with this, we observed that when an excess of nonradioactive ATP was used to chase the phosphoenzyme at 6 ms, the EP level rose briefly before decaying (Figure 4). When dephosphorylation by unlabeled ATP at 6 ms was simulated according to the mechanism given in the legend to Table VI, the rate constants in column 1 (where k_{-1} = 35 s^{-1}), and the assumption that $k_1 = 0$ upon addition of ATP (i.e., that further binding of labeled ATP is prevented by the cold ATP chase), the qualitative behavior of the reaction was reproduced (dashed curve, Figure 4), but the overshoot was too large. A better fit (solid curve, Figure 4) was obtained by allowing the ATP dissociation rate constant (k_{-1}) to increase from 35 to 250 s^{-1} during dephosphorylation. A similar problem arose in trying to simulate the behavior of the ADP-induced dephosphorylation reaction at 6 ms (dashed curve, Figure 3). To reproduce the observed time dependence, it was necessary to readjust $k_2 = 0$ or $k_{-1} \geq 3000$ s^{-1} at the start of dephosphorylation which resulted in rapid depletion of the pool of bound nucleotide. Similar adjustments in k_{-1} were unnecessary for simulating ADP-induced dephosphorylation at 116 ms because by that point in time the conversion of EATP to phosphoenzyme is virtually complete. The high values for k_{-1} needed to fit the

[3] J. P. Froehlich and P. F. Heller, unpublished results.

transient-state time dependence of the ATP-induced and ADP-induced dephosphorylation reactions are clearly too large to allow significant phosphorylation of the enzyme to occur at the low ATP levels employed in these studies.

*Comparison of the Transient Time Courses of E*P Formation and Intravesicular Ca^{2+} Accumulation.* If phosphoenzyme isomerization is the rate-limiting step in the Ca^{2+} translocation sequence, then intravesicular Ca^{2+} accumulation should show a similar time dependence to E*P formation during the initial phase of the reaction. To test this hypothesis, we compared the initial time course of E*P formation with that of intravesicular Ca^{2+} accumulation determined by incubating vesicles with ATP and $^{45}Ca^{2+}$ for a short time and later adding EGTA + ADP to prevent further uptake (Sumida & Tonomura, 1974; Ikemoto et al., 1981b). In the presence of ADP, Ca^{2+} bound to EP is released to the external medium as a consequence of reversal of steps 1, 2, and 3 (Scheme I), whereas Ca^{2+} associated with E*P will either be released to the outside or be transported to the inside, depending on whether E*P is converted back to EP or hydrolyzed to P_i. Figure 5 shows the initial time course of intravesicular Ca^{2+} accumulation (closed circles) together with the time courses of phosphoenzyme formation (closed triangles) and P_i release (open triangles) measured in an acid quench experiment using the same preparation. As seen in the figure, the intravesicular Ca^{2+} level showed a biphasic time-dependent increase without an initial lag phase. Between 200 and 540 ms, Ca^{2+} accumulation was linear (v = 11 nmol mg^{-1} s^{-1}) while at longer time intervals a progressive decline in the rate was observed (not shown). Extrapolation of the linear portion of the Ca^{2+} uptake curve to zero reaction time gave an intercept value of 1.25–1.5 nmol of Ca^{2+}/mg of protein. The rate constant for the initial phase of Ca^{2+} uptake, obtained by subtracting the contribution of the late phase from the early time points and plotting the difference semilogarithmically, was 15 s^{-1}. Following a lag phase, P_i production increased rapidly during the time interval in which the rate of Ca^{2+} accumulation began to decline. After 100 ms, Ca^{2+} uptake was accompanied by stoichiometric P_i release.

The time course of E*P formation, represented by the dashed curve in Figure 5, was calculated from the product of E^*P/EP_0 given in Table II times the corresponding phosphoenzyme level plotted in Figure 5. The curve gave a reasonably good fit to a single exponential with a rate of 42 s^{-1}. Because this rate is 3 times larger than the initial rate of Ca^{2+} accumulation measured under similar conditions, formation of the ADP-insensitive phosphoenzyme apparently took place prior to release of Ca^{2+} on the inside of the vesicle.

When Ca^{2+} accumulation was terminated by the addition of 2.5 mM EGTA alone, a biphasic response was seen (not shown) which had a zero-time value of 2.6 nmol/mg and closely paralleled the time course of Ca^{2+} uptake obtained by quenching with EGTA + ADP. A similar pattern has been noted by others (Sumida et al., 1978; Ikemoto et al., 1981a) and is qualitatively consistent with the biphasic uptake reported by Pierce et al. (1983) using flash photolysis of caged ATP to trigger Ca^{2+} accumulation. Since the amount of Ca^{2+} uptake determined by quenching with EGTA alone equals the sum of the phosphoenzyme-bound Ca^{2+} plus intravesicular Ca^{2+} (Sumida & Tonomura, 1974; Sumida et al., 1978), the amount of bound Ca^{2+} was 2.6 nmol/mg of protein. This is equivalent to a Ca^{2+}:phosphoenzyme ratio of 1:1 and is consistent with the transport ratio calculated from the steady-state velocities of Ca^{2+} accumulation and ATP hydrolysis (Figure 5).[4]

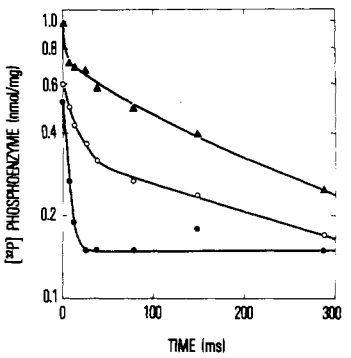

FIGURE 6: Effect of reduced $[K^+]$ and $[Mg^{2+}]$ on ADP-induced dephosphorylation in the presence or absence of a Ca^{2+} jump. The conditions used to phosphorylate the enzyme were identical with those described in the legend to Figure 1 except that the $[K^+]$ was 5 mM and the $[Mg^{2+}]$ adjusted as follows: (▲) 3 mM; (○, ●) 0.1 mM. After 116 ms of phosphoenzyme formation, dephosphorylation was initiated by the addition of (▲, ○) 1.66 mM ADP or (●) 1.66 mM ADP + 5 mM $CaCl_2$.

Calcium Jump Activated Decomposition of the Phosphoenzyme Formed at Low K^+ and Mg^{2+} Concentrations. From the results of the ADP + Ca^{2+} jump experiments in Figure 3 and in Table III, it appears that the low-affinity sites on E*P rapidly become available to bind Ca^{2+} from the external medium, implying that Ca^{2+} dissociation from the transport sites is very fast. Using the fluorescent indicator ANS to monitor intravesicular Ca^{2+} uptake, Chiu & Haynes (1980) showed that by lowering the concentrations of K^+ and Mg^{2+} they were able to suppress the initial rapid increase in fluorescence associated with the first partial turnover of the pump. This suggests that if phosphoenzyme isomerization controls the rate of Ca^{2+} release on the inside of the vesicle, then decreasing $[K^+]$ and $[Mg^{2+}]$ should slow the rate of conversion of EP to E*P.

Figure 6 (open circles) shows the results of a double mixing experiment in which ADP was added to the phosphoenzyme formed by incubating vesicles with 10 μM [γ-^{32}P]ATP for 6 ms in the presence of 5 mM K^+ and 0.1 mM Mg^{2+}. The phosphoenzyme decayed biphasically ($k_{initial}$ = 25 s^{-1}) without evidence of the rapid ADP-sensitive phase observed at higher K^+ and Mg^{2+} concentrations (cf. Figure 3). Preliminary results obtained in this laboratory indicate that both components of dephosphorylation are ADP insensitive, since both phases were accompanied by stoichiometric phosphate production.[3] Upon addition of 5 mM Ca^{2+} + 1.66 mM ADP, only a single rapid phase of dephosphorylation was observed (k = 50 s^{-1}) followed by a stable residual component that accounted for about one-fourth of the phosphoenzyme initially present (closed circles, Figure 6). Because raising the $[Ca^{2+}]$ increased the rate of phosphoenzyme decay, it appears that both components of the dephosphorylation reaction at 6 ms are ADP insensitive and, therefore, that these conditions did not lead to a decrease in the rate of conversion of EP to E*P. It should be noted, however, that the Ca^{2+} jump decay rate constant was reduced (50 s^{-1}) compared to the value obtained at higher Mg^{2+} and K^+ levels (144 s^{-1}; Table I). This suggests that these cations modulate the activity of the back-transition possibly by changing the rate at which the low-affinity sites become exposed to the extravesicular medium.

[4] The transport ratio in these experiments was one Ca^{2+} per ATP on the basis of the results shown in Table II and Figure 5. A similar ratio was obtained by Rossi et al. (1979) under conditions similar to ours (i.e., 10 μM ATP, pH 6.8).

Raising the Mg^{2+} concentration from 0.1 to 3 mM at 5 mM KCl partially restored the sensitivity of the phosphoenzyme to ADP (closed triangles, Figure 6). However, the amplitude of the initial phase was smaller than that obtained with 100 mM KCl, implying that Mg^{2+} concentrations in excess of 0.1 mM may be required to stabilize the formation of EP.

Discussion

In this study, the pattern of dephosphorylation resulting from the addition of ADP to phosphoenzyme formed after a brief exposure to ATP was used to evaluate the rate constants controlling interconversion of the ADP-sensitive and ADP-insensitive phosphoenzymes. At 21 °C, isomerization in the forward direction occurred very rapidly as evidenced by the fact that the level of E*P, expressed as a fraction of the total phosphoenzyme, rose to 85% of its final value 6 ms after the start of phosphorylation. About 40% of the phosphoenzyme formed during that time interval was ADP sensitive, indicating that ADP rapidly dissociates from the catalytic site following phosphoryl group transfer. Further proof that E*P formation occurs rapidly following transphosphorylation was obtained from computer simulations of ADP-induced dephosphorylation using Scheme I (Table VI). Using 1000 s^{-1} for the rate of ADP dissociation, it was necessary to assign the forward rate of isomerization a value of 500 s^{-1} in order to obtain a satisfactory fit to the phosphoenzyme decay curve at 6 ms. This may be compared to the rate constant for E*P formation calculated from the relationship between the overall reaction velocity, v, and the steady-state concentrations of phosphorylated intermediates (see Scheme I):

$$v = k_4[EP] - k_{-4}[E^*P]$$

Substituting v = 11 nmol mg^{-1} s^{-1}, k_{-4} = 10 s^{-1}, and the concentrations of EP and E*P measured at 116 ms (Table I) into the above expression yields k_4 = 32 s^{-1}. The marked dissimilarity between the transition rate constants evaluated from the transient- and steady-state phases of the ATPase reaction indicates the presence of complex behavior that results in apparent slowing of the isomerization reaction prior to completion of the first turnover (see below).

Takisawa & Makinose (1983) have recently shown that an approximate time-dependent correlation exists between Ca^{2+} release and E*P formation at 0 °C in the deoxycholate-solubilized CaATPase. They also found that E*P decay and P_i release resulting from the addition of ADP were stoichiometrically related. In contrast, our results obtained at 21 °C with the vesicular preparation indicate that intravesicular Ca^{2+} accumulation is delayed with respect to E*P formation (Figure 5), implying that Ca^{2+} dissociation from the ADP-insensitive phosphoenzyme is slow, contrary to expectations for a low-affinity binding site.[5] There is growing evidence that during translocation, Ca^{2+} becomes occluded upon formation of the ADP-insensitive phosphoenzyme (Takakuwa & Kanazawa, 1979, 1982; Dupont, 1980; Takisawa & Makinose, 1981, 1983; Pierce et al., 1983). If the conformational transition that releases occluded Ca^{2+} at the inner membrane surface were to take place *after* phosphoenzyme isomerization and at a much slower rate, this could account for the dissimilarity in the rates of E*P formation and Ca^{2+} release. This is shown in the following scheme:

$$EP(Ca) \rightleftharpoons E^*P(Ca) \rightleftharpoons E^*P\overset{Ca^{2+}}{Ca} \rightleftharpoons E^*P \rightleftharpoons E^*\cdot P_i$$

where the parentheses around Ca^{2+} designate an occluded form of the cation. The sequence shows only one Ca^{2+} occluded per phosphorylation site since at low ATP levels Ca^{2+} uptake is approximately stoichiometric with P_i release in the steady state (Figure 5). Following the isomerization step, only a small fraction of the occluded Ca^{2+} will remain bound to the transport site due to the decrease in the affinity of the carrier for Ca^{2+}. Since E*P(Ca) breaks down at a comparatively slow rate ($\sim$15 s^{-1}), the Ca^{2+} concentration in the vicinity of the transport site will tend to remain high following Ca^{2+} dissociation. Upon addition of ADP, a portion of this Ca^{2+} will occupy the transport site, activating the conversion of E*P to EP and preventing P_i release from becoming stoichiometric with E*P decay (Figure 1; Table I). Inesi et al. (1982) proposed that steps associated with Ca^{2+} release may control the rate of E*P hydrolysis on the basis of a comparison of the kinetics of P_i production measured under turnover conditions and following a pH jump. They also noted changes in transient P_i release following enzyme solubilization that were compatible with the removal of structural constraints preventing immediate Ca^{2+} release (Kosk-Kosicka et al., 1983). In terms of the above reaction scheme, the effects produced by detergent can be explained by assuming that solubilization of the enzyme destabilizes E*P(Ca), causing acceleration of the rates of Ca^{2+} and P_i release.

Consistent with the predictions of Scheme I, intravesicular Ca^{2+} accumulation during the transient phase of phosphorylation exceeded the formation of inorganic phosphate (Figure 5). Following maximum phosphoenzyme formation, both of these reactions began to decline in activity, indicating that the conformational step that controls Ca^{2+} release during the burst phase is followed by another slow transformation that is rate limiting for ATP hydrolysis and Ca^{2+} transport in the steady state. Although the precise nature of this step is unknown, there is fairly good evidence from rapid quench (Sumida et al., 1978; Scofano et al., 1979) and from $P_i \rightleftharpoons H^{18}OH$ exchange experiments (McIntosh & Boyer, 1983) that it corresponds to the E* to E transition. This step has also been implicated in recycling of the transport sites to the extravesicular surface following Ca^{2+} release inside the vesicle (Carvahlo et al., 1976; de Meis & Vianna, 1979). Although this interpretation is consistent with reports that leaky vesicles can synthesize ATP in the absence of a gradient (Knowles & Racker, 1975; de Meis & Tume, 1977), it is clear from the results presented in Table IV that increased membrane permeability to Ca^{2+} is not an essential requirement for activating the conversion of E*P to EP. On the other hand, adding high concentrations of Ca^{2+} alone did not immediately inhibit the breakdown of E*P to P_i unless the ionophore was also present (Table V). Taken together, these results suggest that ADP binding triggers a conformational change in the carrier that exposes the low-affinity Ca^{2+} binding sites to the external medium and that in the absence of ADP these sites return to the extravesicular surface following the hydrolysis of E*P. It should be noted that since the phosphorylated carrier can bind Ca^{2+} either from the external medium (Ca^{2+} jump) or from the membrane (occluded Ca^{2+}), these sites presumably have access to both compartments when ADP is present. The mechanism by which this is accomplished is difficult to envision but may involve rapid alternation of the transport sites between the two locations, similar to the shuttle mechanism proposed by Chiesi & Wen (1983) to explain rapid

[5] Assuming the discharge site has a $K_d \simeq 1$ mM (Table II) and that the rate constant for Ca^{2+} binding is between 10^6 and 10^8 M^{-1} s^{-1} (Hammes & Schimmel, 1970), the rate constant for Ca^{2+} dissociation is >1000 s^{-1}.

Ca^{2+} release mediated by the phosphorylated carrier in the absence of Mg^{2+}.

Lowering the K^+ and Mg^{2+} concentrations, while altering the pattern of ADP-induced dephosphorylation, did not slow the rate of phosphoenzyme isomerization (Figure 6). Since these conditions have been shown to substantially reduce the amount of Ca^{2+} uptake during the initial turnover of the pump (Chiu & Haynes, 1980), Ca^{2+} evidently remains bound to the carrier after isomerization despite the large decrease in Ca^{2+} binding affinity that accompanies this transition. These results lend additional support to the above scheme and suggest that the gating mechanism controlling the release of Ca^{2+} inside the vesicle is activated by K^+ and Mg^{2+} ions. Since the initial rate of P_i production depends on how rapidly Ca^{2+} leaves the occluded state, this could in part explain the accelerating effect these ions have on hydrolysis of the ADP-insensitive phosphoenzyme (Shigekawa & Akowitz, 1979; Yamada & Ikemoto, 1980).

In addition to the time delay between E*P formation and Ca^{2+} release, there were three additional features of the pre-steady-state kinetic behavior that are incompatible with the quantitative predictions of Scheme I. First, addition of ADP 6 ms after initiation of phosphorylation produced a rapid phase of dephosphorylation ($k_{-2} > 300\ s^{-1}$) contrary to expectations that the initial decay rate would be slowed by continued phosphorylation from the bound nucleotide pool (dashed line, Figure 3). This implies that ADP, in addition to reversing phosphorylation, rapidly inhibits phosphoenzyme formation, possibly by binding to a separate modifier site that activates ATP dissociation from the catalytic site. Chasing with unlabeled ATP produced a similar but less pronounced effect on phosphoenzyme decomposition at 6 ms (Figure 4) which suggests that the same modifier site may also accommodate ATP.

Second, both the rate of ADP-induced E*P decay (Table I) and the degree of cooperative interaction between low-affinity Ca^{2+} binding sites (Table III) decreased as a function of increasing phosphorylation time. Since the level of phosphorylation was also changing during this interval, it is possible that the observed changes in behavior are related to a change in the number of catalytic sites phosphorylated. This requires that phosphorylated and unphosphorylated carriers be allowed to interact during the transport cycle, implying that the minimum functional unit is an oligomer.

The third observation that is inconsistent with Scheme I concerns the previously noted discrepancy between the rates of E*P formation calculated from the pre-steady-state and steady-state kinetic results. From the values for the initial rate of E*P formation ($500\ s^{-1}$) and its rate of conversion back to EP ($10\ s^{-1}$), we expected the steady-state ratio of EP to E*P to be less than 0.1, whereas the actual ratio was about 0.5 (Table I). The unexpectedly high steady-state level of EP cannot be attributed to the presence of a rapid equilibrium between EP and E*P because that would result in a very rapid decay of E*P following the addition of ADP. This behavior cannot be explained by assuming that the EP state is rapidly repopulated on the second turnover since this would require an abnormally high steady-state rate of ATP hydrolysis and eliminate the early lag in P_i production (Figure 5). A more likely explanation, based on the CaATPase dimer model proposed by Ikemoto and co-workers (Ikemoto et al., 1981a,b), assumes that phosphorylation of the enzymes is governed by a mechanism in which half of the subunits are one step ahead of the other half in carrying out phosphoenzyme formation. If this coupling relationship is maintained throughout the entire cycle, the enzyme will form an intermediate in which the ADP-sensitive and ADP-insensitive phosphoenzymes occur on adjacent subunits (designated by the unprimed and primed superscripts, respectively) as shown below:

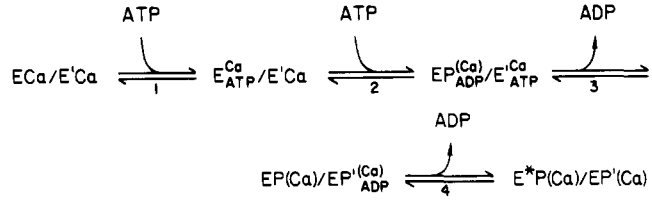

Because the coupled forward reactions leading to the mixed final state are fast, conversion of EP to E*P in the unprimed subunit will occur immediately upon addition of ATP to the Ca^{2+}-loaded enzyme. Enzyme will accumulate in the final state if phosphoenzyme isomerization occurring in the primed subunit is controlled by a slow transformation in the unprimed subunit:

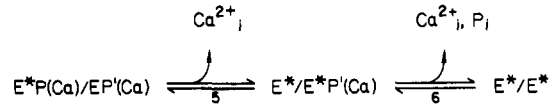

Here, it is assumed that release of occluded Ca^{2+} from E*P-(Ca) is slow and prevents EP from being rapidly converted to E*P in the adjacent subunit. If release of the second Ca^{2+} ion occurs more slowly than the first, then the time courses of Ca^{2+} accumulation and P_i release will be biphasic (Figure 5), and both E*P(Ca)/EP'(Ca) and E*/E*P'(Ca) will accumulate, resulting in a steady-state ratio of ADP-sensitive and ADP-insensitive phosphoenzymes similar to the observed (1:2) distribution.

Although the dimer mechanism predicts the correct steady-state ratio of the ADP-sensitive and ADP-insensitive intermediates, it does not yield the observed pattern of dephosphorylation produced by ADP without making additional assumptions about the intersubunit coupling mechanism. According to the scheme, rapid complexation of ADP with EP'Ca (reversal of step 4) will induce an equally rapid conversion of E*P(Ca) back to EP(Ca) if the active-site coupling is strong. This would in turn lead to rapid dephosphorylation of both subunits by reversal of steps 2 and 3 and eliminate the appearance of the slow phase of dephosphorylation which follows the addition of ADP. To reproduce the observed pattern of phosphoenzyme decay, the scheme must be modified to allow weak coupling between the subunits up to the point where the second mole of ADP is released. Alternatively, ADP binding may weaken the subunit–subunit interaction, permitting EP and E*P to dephosphorylate independently.

The dimer mechanism predicts that there will be two sources of P_i production resulting from E*P hydrolysis occurring in adjacent subunits. For the case in which the dephosphorylation rate constants corresponding to the two pathways are unequal, the resulting time course of EGTA-induced phosphoenzyme decomposition will exhibit biphasic kinetics. Such behavior has been previously observed by us (Sumida et al., 1980) and is also apparent in the dephosphorylation experiment shown in the inset to Figure 4 (EGTA or 0.5 mM ATP chase). Compared to EGTA, chasing the phosphoenzyme with 5 mM ATP caused both the fast and slow components to disappear more rapidly (Figure 4), indicating that ATP, like K^+ and Mg^{2+}, can activate E*P hydrolysis (Shigekawa & Dougherty, 1978; Dupont, 1980). Since Ca^{2+} release from E*P(Ca) controls the rate of E*P hydrolysis, it follows that ATP should act by increasing the rate at which Ca^{2+} leaves the occluded

state. This would presumably be mediated by interaction of ATP with a weak binding site on the phosphorylated carrier and is similar to the mechanism proposed by Post et al. (1972) to account for the effect high concentrations of ATP have on the rate of release of K^+ from the occluded K^+ form of the (Na,K)-ATPase.

ACKNOWLEDGMENTS

We are grateful to Dr. Robert L. Post for helpful discussions and Dana A. Jarvis and Miriam J. Glaser for their assistance in preparing the manuscript.

Registry No. ATPase, 9000-83-3; ADP, 58-64-0; Ca, 7440-70-2.

REFERENCES

Bastide, F., Meissner, G., Fleischer, S., & Post, R. L. (1973) *J. Biol. Chem. 248*, 8385–8391.

Bulos, B. A., & Sacktor, B. (1979) *Anal. Biochem. 95*, 62–72.

Carvahlo, M. G. C., Souza, D. O., & de Meis, L. (1976) *J. Biol. Chem. 251*, 3629–3636.

Chiesi, M., & Wen, Y. (1983) *J. Biol. Chem. 258*, 6078–6085.

Chiu, V. C. K., & Haynes, D. H. (1980) *J. Membr. Biol. 56*, 219–239.

de Meis, L. (1981) in *Transport in the Life Sciences* (Bittar, E., Ed.) Vol. II, pp 1–163, Wiley, New York.

de Meis, L., & Tume, R. (1977) *Biochemistry 16*, 4455–4463.

de Meis, L., & Vianna, A. L. (1979) *Annu. Rev. Biochem. 48*, 275–292.

Dupont, Y. (1980) *Eur. J. Biochem. 109*, 231–238.

Dupont, Y. (1982) *Biochim. Biophys. Acta 688*, 75–87.

Froehlich, J. P., & Taylor, E. W. (1975) *J. Biol. Chem. 250*, 2013–2021.

Froehlich, J. P., & Taylor, E. W. (1976) *J. Biol. Chem. 251*, 2307–2315.

Froehlich, J. P., Sullivan, J. V., & Berger, R. L. (1976) *Anal. Biochem. 73*, 331–341.

Froehlich, J. P., Heller, P. F., & Passonneau, J. V. (1981) *Fed. Proc., Fed. Am. Soc. Exp. Biol. 39*, 2151.

Frost, A. A., & Pearson, R. G. (1985) in *Kinetics and Mechanism*, 2nd ed., pp 1–405, Wiley, New York.

Hammes, G. G., & Schimmel, P. R. (1970) *Enzymes, 3rd Ed. 2*, 67–114.

Ikemoto, N. (1975) *J. Biol. Chem. 250*, 7219–7224.

Ikemoto, N. (1976) *J. Biol. Chem. 251*, 7275–7277.

Ikemoto, N., Garcia, A. M., Kurobe, Y., & Scott, T. L. (1981a) *J. Biol. Chem. 256*, 8593–8601.

Ikemoto, N., Miyao, A., & Kurobe, Y. (1981b) *J. Biol. Chem. 256*, 10809–10814.

Inesi, G., Kurzmack, M., & Verjovski-Almeida, S. (1978) *Ann. N.Y. Acad. Sci. 307*, 224–227.

Inesi, G., Kurzmack, M., Kosk-Kosicka, D., Lewis, D., Scofano, H. M., & Guimaraes-Motta, H. (1982) *Z. Naturforsch., C: Biosci. 37C*, 685–691.

Kanazawa, T., & Boyer, P. D. (1973) *J. Biol. Chem. 248*, 3163–3172.

Kanazawa, T., Yamada, S., Yamamoto, T., & Tonomura, Y. (1971) *J. Biochem. (Tokyo) 70*, 95–123.

Knott, G. D. (1979) *Comput. Programs Biomed. 10*, 271–280.

Knowles, A. F., & Racker, E. (1975) *J. Biol. Chem. 250*, 1949–1951.

Kosk-Kosicka, D., Kurzmack, M., & Inesi, G. (1983) *Biochemistry 22*, 2559–2567.

Kurzmack, M., Verjovski-Almeida, S., & Inesi, G. (1977) *Biochem. Biophys. Res. Commun. 78*, 772–776.

Lowry, O. H., Rosebrough, N. J., Farr, A. L., & Randall, R. J. (1951) *J. Biol. Chem. 193*, 265–275.

Makinose, M. (1969) *Eur. J. Biochem. 10*, 74–82.

Makinose, M. (1973) *FEBS Lett. 37*, 140–143.

Masuda, H., & de Meis, L. (1973) *Biochemistry 12*, 4581–4585.

McIntosh, D. B., & Boyer, P. D. (1983) *Biochemistry 22*, 2867–2875.

Pickart, C. M., & Jencks, W. P. (1982) *J. Biol. Chem. 257*, 5319–5322.

Pierce, D. H., Scarpa, A., Topp, M. R., & Blaise, J. K. (1983) *Biochemistry 22*, 5254–5261.

Post, R. L., Hegyvary, C., & Kume, S. (1972) *J. Biol. Chem. 247*, 6530–6540.

Rossi, B., Leone, F. A., Gache, L., & Lazdunski, M. (1979) *J. Biol. Chem. 254*, 2302–2307.

Scofano, H. M., Vieyra, A., & de Meis, L. (1979) *J. Biol. Chem. 254*, 10227–10231.

Shigekawa, M., & Dougherty, J. P. (1978) *J. Biol. Chem. 253*, 1458–1464.

Shigekawa, M., & Akowitz, A. A. (1979) *J. Biol. Chem. 254*, 4726–4730.

Shigekawa, M., & Kanazawa, T. (1982) *J. Biol. Chem. 257*, 7657–7665.

Shigekawa, M., Dougherty, J. P., & Katz, A. M. (1978) *J. Biol. Chem. 253*, 1442–1450.

Sumida, M., & Tonomura, Y. (1974) *J. Biochem. (Tokyo) 75*, 283–297.

Sumida, M., Wang, T., Mandel, F., Froehlich, J. P., & Schwartz, A. (1978) *J. Biol. Chem. 253*, 8772–8777.

Sumida, M., Wang, T., Schwartz, A., Younkin, C., & Froehlich, J. P. (1980) *J. Biol. Chem. 255*, 1497–1503.

Tada, M., Yamamoto, T., & Tonomura, Y. (1978) *Physiol. Rev. 58*, 1–79.

Takakuwa, Y., & Kanazawa, T. (1979) *Biochem. Biophys. Res. Commun. 27*, 1209–1216.

Takakuwa, Y., & Kanazawa, T. (1982) *J. Biol. Chem. 256*, 426–431.

Takisawa, H., & Makinose, M. (1981) *Nature (London) 298*, 271–273.

Takisawa, H., & Makinose, M. (1983) *J. Biol. Chem. 258*, 2986–2992.

Yamada, S., & Tonomura, Y. (1972) *J. Biochem. (Tokyo) 72*, 417–425.

Yamada, S., & Ikemoto, N. (1980) *J. Biol. Chem. 255*, 3108–3119.